

Polynomial C^2 spline surfaces guided by rational multisided patches

Kęstutis Karčiauskas¹ and Jörg Peters²

¹ Vilnius University, Vilnius 03225, Lithuania,
kestutis.karciauskas@maf.vu.lt,

WWW home page: <http://www.mif.vu.lt/cs2/cagl/>

² University of Florida, Gainesville, FL 32611, USA
jorg@cise.ufl.edu,

WWW home page: <http://www.cise.ufl.edu/~jorg/>

Abstract. An algorithm is presented for approximating a rational multi-sided M-patch by a C^2 spline surface. The motivation is that the multi-sided patch can be assumed to have good shape but is in nonstandard representation or of too high a degree. The algorithm generates a finite approximation of the M-patch, by a sequence of patches of bidegree (5, 5) capped off by patches of bidegree (11, 11) surrounding the extraordinary point.

The philosophy of the approach is (i) that intricate reparametrizations are permissible if they improve the surface parametrization since they can be precomputed and thereby do not reduce the time efficiency at runtime; and (ii) that high patch degree is acceptable if the shape is controlled by a guiding patch.

1 Introduction

When constructing C^2 spline surfaces using a finite number of tensor-product Bézier patches such as [4, 11, 13, 7], the shape is often unsatisfactory near extraordinary points where more or less than four patches meet since the curvature is not evenly distributed or shows local extrema not implied by the surrounding data [10]. For subdivision schemes, the cause of shape artifacts has recently been analyzed and made explicit (see [9], [6]).

By contrast, rational multisided M-patches [5], joined smoothly to a surrounding B-spline complex, appear to consistently yield good shape. This paper does not verify the empirical observation of good shape but explores the technical challenge of how to transfer a good M-patch into a standard spline framework.

M-patches are rational and can therefore be represented as a collection of rational tensor-product Bézier subpatches. If the number of sides is 5 or 6, a variant of the M-patch can be represented as a collection of rational tensor-product Bézier patches of bidegree (8, 8). But for a general m -sided M-patch, the bidegree is $(4(m-2), 4(m-2))$.

The idea pursued in this paper is to capture the shape of the M-patch with a C^2 approximation of moderate bidegree. We describe a finite approximation of the M-patch, by a sequence of patches of bidegree (5, 5) but with patches adjacent to the extraordinary point of bidegree (11, 11). A key point is the definition of reparametrizations that improve the surface parametrization when approximating the M-patch. These reparametrization, maps $\mathbb{R}^2 \rightarrow \mathbb{R}^2$, decompose the domain m -gon into C^2 -connected

annuli or rings and a central piece. The surface approximation consists correspondingly of nested annuli and a final cap. Each annulus and the cap pick up second order Hermite data from the M-patch.

The bidegree of the central, extraordinary patches is still high, but all experiments with constructions of lower the bidegree have so far resulted in a considerably reduction of the surface quality. The paper focuses on the technical challenge of creating a C^2 surface that Hermite-interpolates a given M-patch.

One of the key ideas, construction of good reparametrizations and composition with a polynomial patch that determines the shape is a logical extension of similar ideas proposed in [11, 13, 7].

The paper is organized as follows.

Section 2 defines M-patches and the transition of the M-patch to an existing spline complex.

Section 3 defines the transitional reparametrizations and the patches of bidegree (5, 5).

Section 4 describes the cap of patches of bidegree (11,11) that approximates the M-patch near the extraordinary point.

The exposition expects familiarity with standard representations of geometric design. The tensor-product Bernstein-Bézier and (uniform) B-spline representations (see [1, 3, 12]) have the form $\sum_{i=0}^{d_1} \sum_{j=0}^{d_2} c_{ij} b_i^{d_1}(u) b_j^{d_2}(v)$, where b_i^d is the i th basis function. In the case of the Bernstein-Bézier form, $b_i^d(u) := \binom{d}{i} (1-u)^{d-i} u^i$. In particular, one can choose the domain as a unit square and then associate layers of coefficients c_{ij} , $j \leq k$ with k th derivatives perpendicular to an edge of the square. In the following, we will often refer to *the three boundary layers* of a polynomial to mean the layers of coefficients c_{ij} , $j \leq 3$ that determine position, first and second derivative across a boundary. Catmull-Clark subdivision [2] generalizes the refinement of bicubic uniform splines to control nets with nodes of arbitrary valence as illustrated in Fig. 1

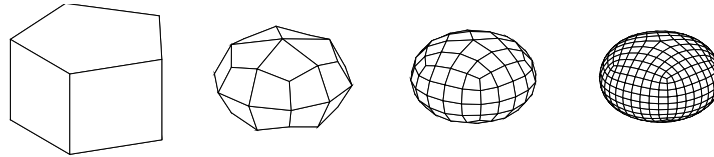


Fig. 1. Three steps of Catmull-Clark subdivision.

2 M-patches and their tensor-border

In this section, we review the construction of rational multi-sided patches, called M-patches [5]. First, M-patches are defined. Then a control structure, called tensor-border, is defined that mimicks the behavior of tensor-product patches along the boundary. Such

a control structure can be derived from an M-patch by combining M-patch basis functions as in [5] or, as in our context, by reparametrization. A third subsection sketches such a reparametrization. That is, the M-patch composed with the reparametrization has tensor-border structure, suitable for smoothly joining the patch to an existing spline complex and filling an m -sided hole.

2.1 Definition of M-patches

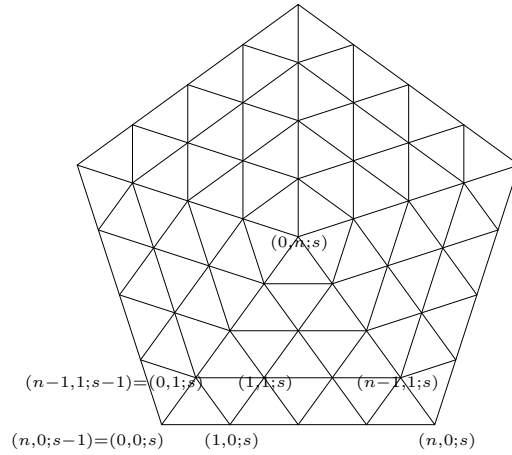


Fig. 2. A nested polygon net \mathcal{NP}_5^n .

Let P_m be a regular m -gon, $m > 4$, with center $\mathbf{0}$ and vertices

$$\mathbf{v}_s := (\cos s\alpha, \sin s\alpha), \quad \alpha = 2\pi/m, s = 0, 1, \dots, m-1.$$

Subscripts are assigned in a cyclic fashion, e.g. $\mathbf{v}_{s+1} = \mathbf{v}_0$ if $s = m-1$ and $\mathbf{v}_{s-1} = \mathbf{v}_{m-1}$ if $s = 0$. We abbreviate $c := \cos \alpha$.

An m -sided *nested polygon net* \mathcal{NP}_m^n of depth n is a set of points in \mathbb{R}^2 ,

$$\frac{n-i-j}{n}\mathbf{v}_s + \frac{i}{n}\mathbf{v}_{s+1} + \frac{j}{n}\mathbf{0}, \quad 0 \leq s \leq m-1, 0 \leq i+j \leq n$$

connected as shown in Fig. 2. That is, each triangle $\Delta \mathbf{v}_s \mathbf{v}_{s+1} \mathbf{0}$ is triangulated in the manner of Greville abscissae of the Bézier form. There are $mn(n+1)/2 + 1$ points in \mathcal{NP}_m^n . It is convenient to refer to the point

$$((n-i-j)\mathbf{v}_s + i\mathbf{v}_{s+1} + j\mathbf{0})/n \quad \text{by the triple } (i, j, s)$$

where $(n-j, j, s-1) = (0, j, s)$.

An edge E_s is a line through the vertices $\mathbf{v}_s, \mathbf{v}_{s+1}$. We set

$$\ell_s(x, y) := -x \cos(s\alpha + \frac{\alpha}{2}) - y \sin(s\alpha + \frac{\alpha}{2}) + \cos \frac{\alpha}{2}.$$

The linear function ℓ_s is zero on the edge E_s and positive at the other points of P_m . The edges E_{s-1} and E_{s+1} intersect at a point \mathbf{k}_s .

Set $C(x, y) = \frac{\cos^2(\alpha/2)}{\cos^2 \alpha} - x^2 - y^2$. The equation $C(x, y) = 0$ defines a circle passing through the points \mathbf{k}_s . For $q = (i, j; s)$ we define

$$f_q := k_{ij}^n g_s^{n-i-j} g_{s+1}^i g^j,$$

where

$$g_s := C \prod_{\sigma \neq s-1, s} \ell_\sigma, \quad g := \prod_{\sigma=0}^{m-1} \ell_\sigma.$$

and k_{ij}^n are positive numbers that satisfy $k_{ij}^n = k_{n-i-j, j}^n$ and $k_{i0}^n = \binom{n}{i}$. Examples are given in [5]. The functions f_q are the *basis functions* of M -patch.

Definition 1. *The m -sided M -patch with the control points $\mathbf{q}_\sigma \in \mathbb{R}^3$ and their weights w_σ , $\sigma \in \mathcal{NP}_m^n$, is the image of the mapping $F : P_m \rightarrow \mathbb{R}^3$ defined by the formula*

$$F = \frac{\sum_{\sigma \in \mathcal{NP}_m^n} w_\sigma \mathbf{q}_\sigma f_\sigma}{\sum_{\sigma \in \mathcal{NP}_m^n} w_\sigma f_\sigma}. \quad (1)$$

2.2 Tensor-border structure

To be able to tie an M -patch into a tensor-product spline complex and fill an m -sided hole, we define a *tensor-border net* with quadrilateral mesh cells. In fact, a tensor-border net is a collection of overlapping quadrilateral nets as shown in Fig. 3. The connectivity and enumeration is as follows.

For fixed integers $m, n, k \leq \lfloor n/2 \rfloor$ an m -sided *tensor-border net* $\mathcal{T}_m(n, k)$ of degree n and order k is indexed by the set of triples

$$[i, j; s], \quad s = 0, \dots, m-1, \quad i = 0, \dots, n, \quad j = 0, \dots, k.$$

The triples are identified via

$$[i, j; s] = [j, n-i; s+1], \quad \text{for } i \geq n-k.$$

Here, we use the notation $[i, j; s]$ to avoid confusion with the subscripts of the basis functions of M -patches.

Definition 2. *A patch F has a tensor-border of order k and of degree n with the vertices \mathbf{q}_σ , $\sigma = [i, j; s] \in \mathcal{T}_m(n, k)$, if, along each edge E_s , it can be locally reparametrized by maps $\rho^{k;s} : \mathbb{R}^2 \rightarrow \mathbb{R}^2$ with parameters (u, t) in such a way that the crossderivatives ∂_t^κ up to order k ,*

$$\left. \frac{\partial^\kappa F \circ \rho^{k;s}}{\partial^\kappa t} \right|_{t=0}, \quad \kappa \leq k,$$

coincide with the crossderivatives of the tensor-product patch of bidegree (n, n) with the control points $\mathbf{q}_{ij} := \mathbf{q}_{[i, j; s]}$.

The reparametrization $\rho^{k;s}$ is defined in the next subsection.

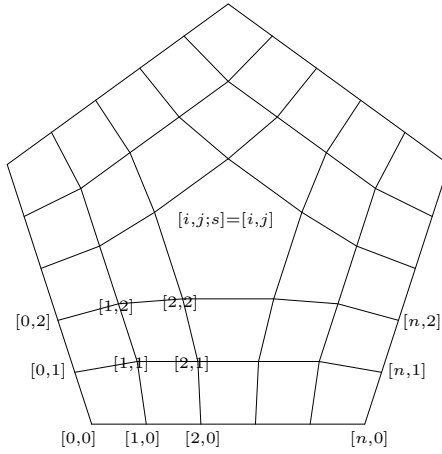


Fig. 3. Tensor-border net of order 2.

2.3 Reparametrizations to form a tensor-border

It is convenient to construct the reparametrizations $\rho^{k;s}$ in Bézier form. Since we are interested in crossderivatives up to order 2, the first three layers of Bézier control points are calculated. We construct the reparametrizations $\rho^{2;s}$ based on two simpler maps $\rho^{0;s}$ and $\rho^{1;s}$, as follows.

- (1) $\rho^{0;s} := \mathbf{v}_s(1 - u) + \mathbf{v}_{s+1}u$ for u on the edge E_s ;
- (2) $\rho^{1;s}$ is of bidegree (3, 3) (see Fig. 4 left) and its Bézier coefficients $\rho_{i0}^{1;s}, i = 0, \dots, 3$ represent $\rho^{0;s}$ in degree-raised form; the coefficients $\rho_{01}^{1;s}$ and $\rho_{31}^{1;s}$ are defined by symmetry; $\rho_{11}^{1;s} := \text{sc}_1 \mathbf{v}_s, \rho_{21}^{1;s} := \text{sc}_1 \mathbf{v}_{s+1}$, where

$$\text{sc}_1 := \frac{3 + 12c + 4c^2 + 8c^3}{9(1 + 2c)}.$$

- (3) $\rho^{2;s}$ is of bidegree (5, 5) (see Fig. 4 right) and its Bézier coefficients $\rho_{ij}^{2;s}, i = 0, \dots, 5, j = 0, 1$, represent $\rho^{1;s}$ in degree-raised form; the coefficients $\rho_{02}^{2;s}, \rho_{12}^{2;s}, \rho_{42}^{2;s}, \rho_{52}^{2;s}$ are defined by symmetry; $\rho_{22}^{2;s} := \text{sc}_2 \mathbf{v}_s, \rho_{32}^{2;s} := \text{sc}_2 \mathbf{v}_{s+1}$, where

$$\text{sc}_2 := \frac{5 + 41c + 129c^2 + 168c^3 + 132c^4 + 120c^5 + 48c^6 + 32c^7}{25(1 + 2c)^3}.$$

Theorem 1. After reparametrization with $\rho^{2;s}$ an M -patch of depth 4 has a tensor-border of order 2 and of degree 7.

The proof is analogous to Proposition 11 of [5].

One further challenge of the construction is that the tensor-border is C^∞ along the domain edge E_s while the corresponding edge in the spline complex is a spline of finite smoothness. The two can be joined by an annulus of patches that match the spline data on the outside and form, along each inside edge, a single polynomial.

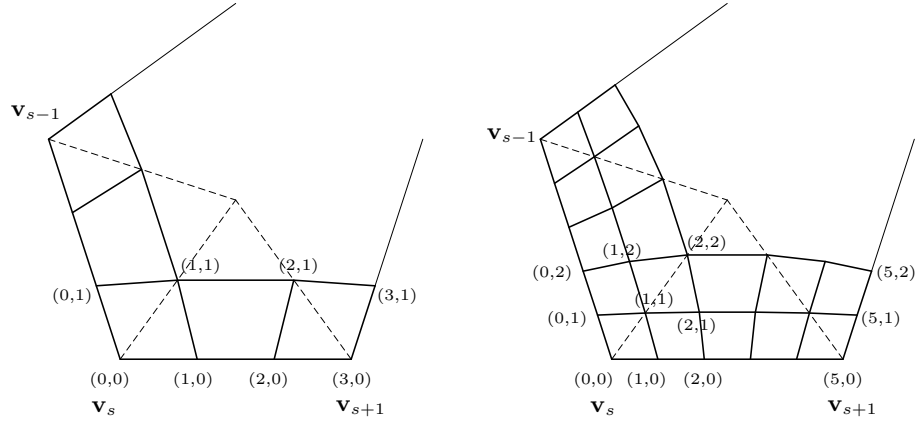


Fig. 4. Reparametrizations of M -patches: $\rho^{1;s}$ for the first cross-derivatives; $\rho^s := \rho^{2;s}$ for the first and second cross-derivatives.

3 Approximating the M -patch by successive annuli of bidegree (5,5)

We now assume that the M -patch has been constructed by fixing the tensor-border to match the given spline complex in a C^2 fashion and fill its m -sided hole. The goal of the following construction is to approximate the M -patch by annuli of the tensor-product patches of bidegree (5, 5). Degree (5, 5) allows matching second order data from an outer annulus and, independently, using three inner layers of Bézier coefficients to pick up second order Hermite data from concentric curves surrounding the central point Q of the M -patch. An infinite sequence of these annuli can be constructed in the spirit of subdivision surfaces, but here we will generate only a few annuli before capping off with the construction detailed in Section 4.

3.1 Outline of the construction

The control points of Bézier patch $G(u, v)$ of bidegree (5,5) are fully determined by the values of its Taylor expansions

$$\partial_u^i \partial_v^j G, \quad 0 \leq i, j \leq 2,$$

at the corners $(0, 0)$, $(1, 0)$, $(0, 1)$, $(1, 1)$. These (Hermite) data are derived by reparametrizing the domain polygon P_m and calculating the derivatives of the reparametrized M -patch. Calculating the derivatives of this composition is a routine job if the reparametrizations is given.

Free parameters are determined by minimizing the following functional.

Definition 3. For a function h with parameters (u, v) in the unit square $I^2 = [0..1]^2$, we define the functional

$$\mathcal{F}_5(h) := \int \int_{I^2} \sum_{i+j=5, i, j \geq 0} \binom{5}{i} (\partial_u^i \partial_v^j h)^2.$$

For a mapping $h = (h_1, h_2) : I^2 \rightarrow \mathbb{R}^2$,

$$\mathcal{F}_5(h) := \mathcal{F}_5(h_1) + \mathcal{F}_5(h_2).$$

3.2 The C^2 transition between the reparametrizations $\rho^{2;s}$ and a bicubic C^2 reparametrization

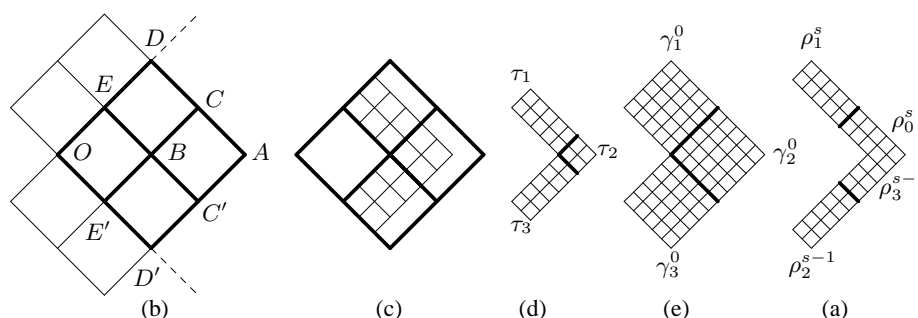


Fig. 5. Three inner layers, corresponding to second-order boundary data, of the bidegree (3,3) reparametrization τ_i are constructed in (b),(c),(d). Three outer layers of the (5,5) partitioned tensor-border reparametrization $\rho^{2;s}$ are shown (a). The reparametrization γ^0 of bidegree (5,5) in Figure (e) is the result of juxtaposing the three inner and outer layers.

The reparametrization $\rho^{2;s} : \mathbb{R}^2 \rightarrow \mathbb{R}^2$ is of bidegree (5,5). This is an unnecessarily high bidegree for forming an m -sided C^2 annulus. Since the bidegree of the innermost patches increases with the degree of the reparametrization, it is convenient to transition to a C^2 annulus of bidegree (3,3) whose properties are well-known and that can be refined by the well-known Catmull-Clark rules.

To transition between the high-degree reparametrization $\rho^{2;s}$ and a (piecewise) bicubic C^2 reparametrization $\tau : \mathbb{R}^2 \rightarrow \mathbb{R}^2$ of the first annulus, a reparametrization γ^0 of bidegree (5,5) is stitched together from the boundary layers of Bézier coefficients of $\rho^{2;s}$ and τ : the outer three layers Hermite-interpolate $\rho^{2;s}$ up to second order and the inner three layers are taken from τ .

If, as is natural, we choose a bicubic τ with m -fold symmetry, we can define its relevant part by five spline control points A, B, C, D, E , each in \mathbb{R}^2 (see Fig. 5 b). Here, we say relevant part, since we only need the innermost three layers of Bézier coefficients of the bicubic annulus for γ^0 . A third annulus would only be needed if we wanted to define the complete bicubic τ . The innermost three layers are defined by a central

spline control point $0 = (0, 0)$ and two surrounding annuli of spline control points. Under symmetry, with A fixed to establish scale, there are a total of 5 scalar degrees of freedom. Due to symmetry, it suffices to describe one sector of γ^0 .

- (a) The reparametrization $\rho^{2;s}(u, v)$ (for $s = 0$) of bidegree $(5, 5)$ is subdivided into four parts

$$\rho_k^s := \rho^{2;s}\left(\frac{k}{4}(1-u) + \frac{1+k}{4}u, \frac{1}{4}v\right), \quad k = 0, \dots, 3.$$

Two pieces ρ_1^s, ρ_0^s of $\rho^{2;s}$ and two pieces of $\rho_3^{s-1}, \rho_2^{s-1}$ of $\rho^{2;s-1}$ form an L -shape. Of this (outer) L -shape, we need only calculate three layers in Bézier form as shown in Fig. 5 a. By construction of $\rho^{2;s}$, the overlap of ρ_0^s and ρ_3^{s-1} is consistent.

- (b,c) The (undetermined) control points A, \dots, E (Fig. 5 b) determine the three boundary layers of a second (inner) L -shape made up of bicubic patches (Fig. 5 c).
 (d) The three layers of Bézier coefficients in (c) are degree-raised to bidegree $(5, 5)$ (Fig. 5 d).
 (e) Now the partial Bézier control nets of the two L shapes constructed in (a) and (d) are simply juxtaposed to form a composite L shape, consisting of three parts $\gamma_1^0, \gamma_2^0, \gamma_3^0$ of bidegree $(5, 5)$ (Fig. 5 e). The control points A, \dots, E are chosen to minimize the functional $\mathcal{F}_5(\tau_1) + \mathcal{F}_5(\tau_2) + \mathcal{F}_5(\tau_3)$ of these parts.

One sector of the first annulus of the biquintic reparametrization γ^0 for $m = 8$ is shown in Fig. 6 as the rightmost triple of patches. By construction, γ^0 is non-singular along inner and outer annulus edges.

3.3 Subsequent annuli of bidegree (5,5)

The first annulus of reparametrizations was created with the help of B -spline control points A, \dots, E . We apply Catmull-Clark subdivision rules to these points and convert the contracting control point nets to contracting annuli of bicubic C^2 -reparametrization γ^k (Fig. 6).

The subdivided B -spline control point nets converge rapidly to the characteristic configuration. The characteristic configuration defines a bicubic annulus γ^c , the characteristic map. At the K th iteration, we transition from γ^K to γ^c using a second single annulus of reparametrizations of bidegree $(5,5)$ that Hermite-blends inner and outer parts of the two annuli exactly as in the construction of γ^0 . The n th subsequent reparametrization can then be chosen as $\gamma^{K+n} = \lambda^n \gamma^c$ where

$$\lambda := \frac{1}{16}(c + 5 + \sqrt{(c+9)(c+1)})$$

is the subdominant eigenvalue of Catmull-Clark subdivision.

From basic facts of Catmull-Clark subdivision, it follows that the constructed reparametrizations γ^k are C^2 within each annulus and join C^2 with adjacent annuli.

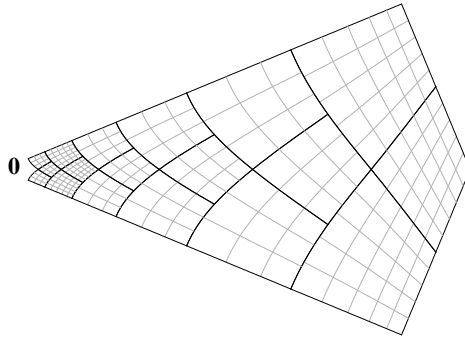


Fig. 6. A sector of the contracting sequence of reparametrizations γ^k . The grey parameter lines reveal the bidegree: $(3, 3)$ except for the outermost layer shown on the right which is of bidegree $(5, 5)$.

3.4 Annuli of Bézier patches

We now construct annuli of Bézier patches of bidegree $(5,5)$ that

- are internally C^2 and join C^2 with the adjacent annuli and that
- approximate the M-patch.

Every reparametrization γ^k is composed with the map F that defines the M-patch. Denote the composition G with parameters (u, v) . Each bidegree $(5, 5)$ patch is constructed as follows.

4	4	4	3	3	3
4	4	4	3	3	3
4	4	4	3	3	3
1	1	1	2	2	2
1	1	1	2	2	2
1	1	1	2	2	2

Fig. 7. Grouping of the Bernstein-Bézier coefficients of a patch of bidegree $(5, 5)$.

- (1) the values of $\partial_u^i \partial_v^j G$ for $0 \leq i, j \leq 2$. are calculated at the vertices $(0, 0)$, $(1, 0)$, $(0, 1)$, $(1, 1)$;
- (2) the calculated data are converted to Bézier form as a part of a patch of bidegree $(5, 5)$;
- (3) the four parts are merged into one patch of bidegree $(5, 5)$ (see Fig. 7);

- (4) the first three layers – marked in Fig. 8 *left* – of a new, inner annulus are replaced by the subdivided C^2 extension of the last three layers – marked in Fig. 8 *right* – of the old, outer annulus.

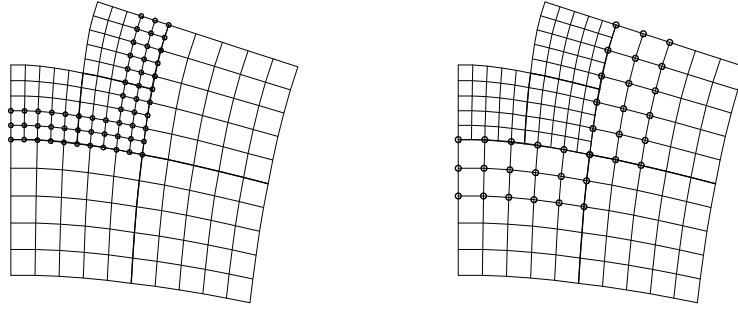


Fig. 8. C^2 extension of the data to inner annulus.

Since the reparametrizations are (parametrically) C^2 and non-singular across patch boundaries,

- the patches are C^2 in each annulus and
- adjacent annuli join C^2 .

Remark 1. If we make the sequence of patches infinite, we obtain a *guided subdivision* construction of degree (5,5). Such a construction can be shown to have a limit point Q , that is the image of the center of the domain polygon under the M-patch. Furthermore, the surface is C^1 and the limit of the tangent planes is the tangent plane of the M-patch at Q . Experiments show that any curvature oscillation is very small. A similar construction of bidegree (6,6) can be shown to be curvature continuous with the limit of Gaussian and mean curvatures equal the corresponding curvatures of the M-patch at Q . However, here, we are concerned only with the finite construction.

4 A spline cap of bidegree (11,11)

In this section, we will develop a ‘cap’ of m patches of bidegree (11, 11) that are G^2 -joined around Q , the central point of the M-patch. While this bidegree is higher than recent C^2 constructions in the literature, it has well-controlled shape. Following the approach from [7], the three boundary layers of the patches are taken from the composition $PW_7 \circ \tilde{\gamma}^s$ where $\tilde{\gamma}^s : \mathbb{R}^2 \rightarrow \mathbb{R}^2$ is a reparametrization and $PW_7 : \mathbb{R}^2 \rightarrow \mathbb{R}^3$ defines the shape. The construction of the relevant layers of the maps is as follows (see Fig.s 9, 11):

- (1) Set

$$\mathbf{v}'_s := \left(\cos \left(s\alpha - \frac{\alpha}{2} \right), \sin \left(s\alpha - \frac{\alpha}{2} \right) \right), \quad \bar{\mathbf{v}}_s := \left(\frac{\cos(s\alpha)}{\cos(\alpha/2)}, \frac{\sin(s\alpha)}{\cos(\alpha/2)} \right).$$

- (2) the (three boundary layers of the) symmetric tensor-product reparametrizations $\tilde{\gamma}^s$ are defined in each sector $\mathbf{v}'_s \mathbf{0} \mathbf{v}'_{s+1}$;
- (3) an auxiliary piecewise C^2 mapping PW_7 of degree 7 is constructed in each of the triangles $\Delta \mathbf{0} \mathbf{v}'_s \bar{\mathbf{v}}_s$ and $\Delta \mathbf{0} \bar{\mathbf{v}}_s \mathbf{v}'_{s+1}$;
- (4) the composition $PW_7 \circ \tilde{\gamma}^s$ is a tensor-product of bidegree $(11, 11)$; its three boundary layers are well-defined from the earlier construction and can be extracted.

We now describe the relevant layers of maps PW_7 and $\tilde{\gamma}^s$ in detail.

4.1 The 135-reparametrizations $\tilde{\gamma}^s$

In this section, we construct the reparametrization $\tilde{\gamma}^s$ shown in Fig. 9. The reparametrization is almost completely pinned down by the requirements that

- $\tilde{\gamma}^s$ is a piece of a control net with m -fold symmetry and
- the i th boundary layer of $\tilde{\gamma}^s$ in Bézier form represents a curve of degree $2i + 1$.

The remaining degrees of freedom are denoted by t_i and are set by minimizing a functional. Note that this calculation is done once and for all and we get specific Bernstein-Bézier coefficients $\tilde{\gamma}_{ij}^s$ that define the first three layers of a polynomial $\tilde{\gamma}^s$ of bidegree $(5, 5)$.

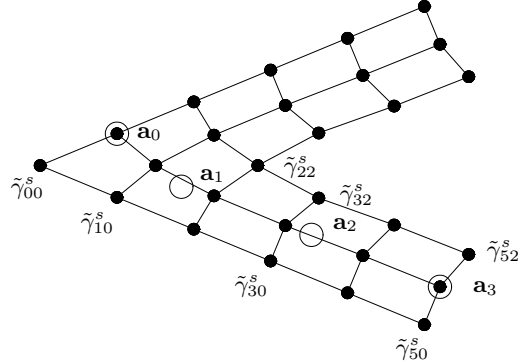


Fig. 9. Boundary layers of Bernstein-Bézier coefficients of the 135-reparametrization $\tilde{\gamma}^s$.

- $\tilde{\gamma}_{i0}^s := (1 - i/5)\mathbf{0} + (i/5)\mathbf{v}'_s$, $i = 0, \dots, 5$; the points $\tilde{\gamma}_{0i}^s$, $i = 1, \dots, 5$, are symmetric to the points $\tilde{\gamma}_{i0}^s$;
- the points $\tilde{\gamma}_{i1}^s$, $i = 0, \dots, 5$, represent a cubic with the control points $\mathbf{a}_0 := \tilde{\gamma}_{01}^s$, $\mathbf{a}_1 := (2/3)\mathbf{0} + (1/3)\mathbf{v}'_s + (1/5)\tan(\alpha/2)\vec{\mathbf{N}}_s$, $\mathbf{a}_2 := (1/3)\mathbf{0} + (2/3)\mathbf{v}'_s + t_0\vec{\mathbf{N}}_s$, $\mathbf{a}_3 := \mathbf{v}'_s + t_1\vec{\mathbf{N}}_s$ in degree-raised form where $\vec{\mathbf{N}}_s := (-\sin(s\alpha - \alpha/2), \cos(s\alpha - \alpha/2))$ is the normal perpendicular to the edge $\bar{\mathbf{v}}_s, \bar{\mathbf{v}}_{s+1}$; the points $\tilde{\gamma}_{1i}^s$, $i = 2, \dots, 5$, are symmetric to the points $\tilde{\gamma}_{i1}^s$;

- $\tilde{\gamma}_{22}^s := (1 - t_2)\mathbf{0} + t_2\bar{\mathbf{v}}_s$, $\tilde{\gamma}_{i2}^s := (1 - t_i)\mathbf{0} + t_i\mathbf{v}'_s + 2(\tilde{\gamma}_{i1}^s - \tilde{\gamma}_{i0}^s)$, $i = 3, \dots, 5$; the points $\tilde{\gamma}_{2i}^s$, $i = 3, \dots, 5$, are symmetric to the points $\tilde{\gamma}_{i2}^s$.

The three boundary layers of the reparametrization just constructed define curves of degree 1, 3 and 5. Therefore $\tilde{\gamma}^s$ is denoted as 135-reparametrization. The reparametrizations $\rho^{2;s}$ from Section 2.3 are also of type 135.

Suppose $R \geq 2$ annuli of Bézier surfaces of bidegree $(5, 5)$ are to be generated before the final cap of bidegree $(11, 11)$. We now fix the free parameters t_i and adjust the contracting reparametrizations of the last two annuli. This procedure is explained below and illustrated for the case $R = 3$ in Fig. 10. As usual, due to symmetry, only one sector need be considered.

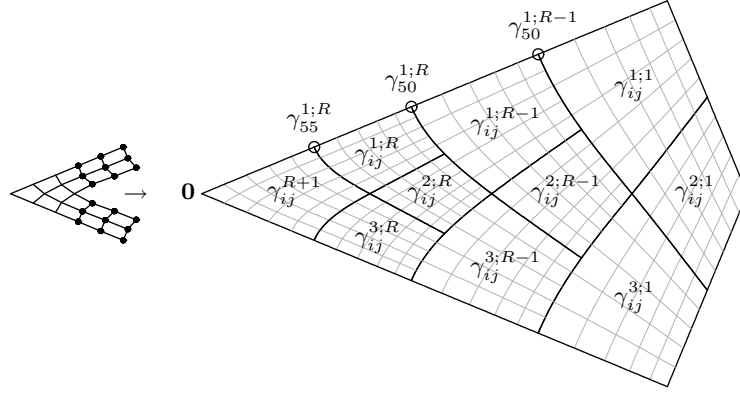


Fig. 10. Finite sequence of reparametrizations.

- (1) The contracting reparametrizations γ^r , defined in Section 3, are degree-raised to bidegree $(5, 5)$; the control points of these reparametrizations are denoted by $\gamma_{ij}^{1;r}$, $\gamma_{ij}^{2;r}$, $\gamma_{ij}^{3;r}$.
- (2) the points $\gamma_{ij}^{k;r}$, $r \leq R - 2$, remain unchanged;
- (3) the part of $\gamma_{ij}^{k;R-1}$ that guarantees a C^2 join to the previous $(R - 2)$ -th annulus remain unchanged;
- (4) the points $\tilde{\gamma}_{ij}^s$ are denoted γ_{ij}^{R+1} ;
- (5) the points $\gamma_{ij}^{1;R}$, $3 \leq i, j \leq 5$, are changed to Hermite-interpolate the three boundary layers of γ_{ij}^{R+1} ; this guarantees a C^2 join between $\gamma^{1;R}$ and γ^{R+1} for those layers; the points $\gamma_{ij}^{3;R}$ are changed analogously;
- (6) the remaining points $\gamma_{ij}^{k;R-1}$, $\gamma_{ij}^{k;R}$ are changed to satisfy the conditions of symmetry and of a C^2 join;
- (7) the reparametrizations defined by the new points $\gamma_{ij}^{k;R-1}$ and $\gamma_{ij}^{k;R}$ are $\gamma^{k;R-1}$ and $\gamma^{k;R}$, respectively; the remaining coefficients of $\gamma^{k;R-1}$ and $\gamma^{k;R}$ and the parame-

ters $t_i, i \in \{0, 1, 3, 4, 5\}$ are determined by minimizing the functional

$$\sum_{k=1}^3 (\mathcal{F}_5(\gamma^{k;R-1}) + \mathcal{F}_5(\gamma^{k;R}));$$

- (8) the points $\gamma_{ij}^{R+1}, 3 \leq i, j \leq 5$, are determined via the C^2 conditions for joining γ^R to γ^{R+1} .
- (9) the parameter t_2 is calculated by minimizing a functional $\mathcal{F}_5(\gamma^{R+1})$, where γ^{R+1} is the reparametrization controlled by the points $\gamma_{ij}^{R+1}, 0 \leq i, j \leq 5$.

4.2 A total degree 7 C^2 approximation of the geometry

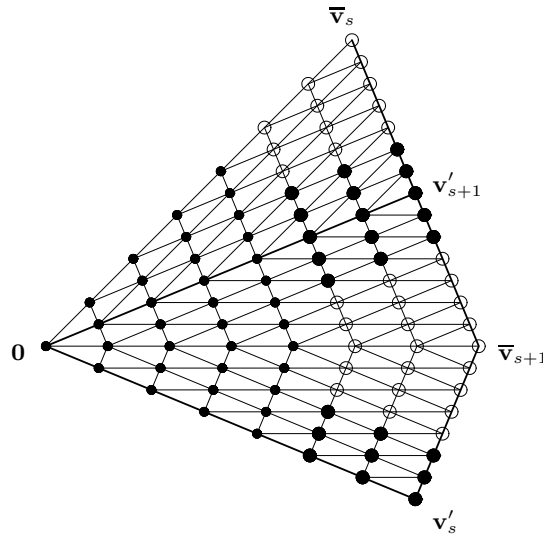


Fig. 11. Schematic view of the Bernstein-Bézier coefficients of three pieces of the auxiliary mapping PW_7 of total degree 7.

The sector $\mathbf{v}'_s \mathbf{0} \mathbf{v}'_{s+1}$ is split into the triangles $\Delta \mathbf{0} \mathbf{v}'_s \bar{\mathbf{v}}_s$ and $\Delta \mathbf{0} \bar{\mathbf{v}}_s \mathbf{v}'_{s+1}$. The control points of a piecewise C^2 mapping PW_7 of degree 7 over $\Delta \mathbf{0} \mathbf{v}'_s \bar{\mathbf{v}}_s$, respectively over $\Delta \mathbf{0} \bar{\mathbf{v}}_s \mathbf{v}'_{s+1}$, are denoted by \mathbf{q}_{ijk}^{2s} and $\mathbf{q}_{ijk}^{2s+1}, i + j + k = 7$. The common central point is $\mathbf{q}_{700}^{2s} = \mathbf{q}_{700}^{2s+1}$.

Let $rep := u\gamma_{50}^{R+1} + v\gamma_{05}^{R+1} + (1 - u - v)\mathbf{0}$ and $G = F \circ rep$, where F defines the M-patch. The values of

$$\partial_u^i \partial_v^j G, \quad 0 \leq i + j \leq 4 \quad \text{at } (0, 0)$$

are calculated and converted to Bézier form of total degree 4. These define a quartic mapping T_4 . The points \mathbf{q}_{ijk}^s , $i \geq 3$, (in Fig. 11 marked as the small disks) are control points of T_4 after raising the degree to 7.

The remaining control points insure a C^2 join between adjacent sectors and are marked as big disks in Fig. 9. For these points the conditions of C^2 join are the same as for the control points of tensor-product surfaces. They are uniquely determined by the requirement that data derived from $PW_7 \circ \tilde{\gamma}^s$ be joined C^2 to the patches of bidegree $(5, 5)$ from the R -th annulus.

The control points marked as the circles do not affect the construction.

Remark 2. Splitting the sector $\mathbf{v}'_s \mathbf{v}'_{s+1}$ into the triangles $\triangle \mathbf{0} \mathbf{v}'_s \bar{\mathbf{v}}_s$ and $\triangle \mathbf{0} \bar{\mathbf{v}}_s \mathbf{v}'_{s+1}$ simplifies the intermediate expressions so that a computer algebra system can derive explicit formulas.

4.3 Capping patches of bidegree $(11, 11)$

We now describe how the Bézier patches G_Q^s , $s = 1, \dots, m$ of bidegree $(11, 11)$ are constructed that cap off the construction at the extraordinary point Q .

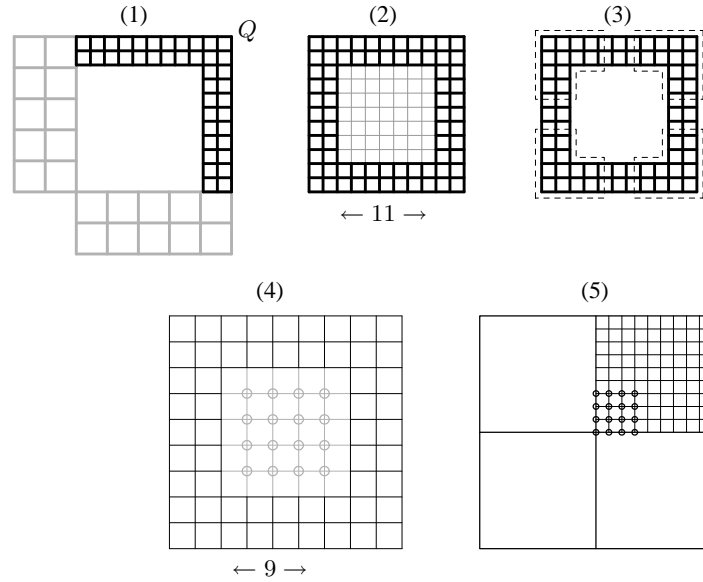


Fig. 12. Construction of the capping patch G_Q^s .

The cross-derivatives of $PW_7 \circ \tilde{\gamma}^s(u, v)$,

$$PW_7 \circ \tilde{\gamma}^s|_{v=0}, \quad (PW_7 \circ \tilde{\gamma}^s)_v|_{v=0}, \quad (PW_7 \circ \tilde{\gamma}^s)_{vv}|_{v=0}$$

are of degrees 7, 9 and 11 respectively. For each edge of G_Q^s emanating from Q , this data defines the first three layers of Bézier coefficients so that G_Q^{s-1} and G_Q^s are joined

with curvature continuity, i.e. the cap is internally curvature continuous. Fig. 12 (1) shows these layers colored black.

The data of the ordinary patches from the R -th annulus, adjacent to the extraordinary patches, are colored grey. These data, degree-raised to bidegree (11, 11) and C^2 extended, define three new layers for the remaining two edges of G_Q^s that are not connected to Q . The cap is thereby joined C^2 to the innermost ordinary annulus.

In Fig. 12 (2), the layers of both types are colored black while the remaining 36 inner control points \mathbf{q}_{ij} , $3 \leq i, j \leq 8$ are colored grey. These 36 inner control points are determined by the guiding M-patch as follows.

- The four corners of already defined control points (marked in Fig. 12 (3) by the dashed lines) are each rerepresented in bidegree (9, 9) form;
- the degree-decreased corners are connected to form a part of a patch of bidegree (9, 9); this part is displayed via black lines in Fig. 12 (4);
- the remaining 16 inner control points $\mathbf{q}_{i,j}^9$ (marked as grey circles in Fig. 12 (4)) are in 1 – 1 correspondence to the 16 corner control points of one quarter \tilde{G} of the patch; these corner control points are marked in Fig. 12 (4) as the black circles and in turn they are defined by the values of

$$\partial_u^i \partial_v^j \tilde{G}, \quad 0 \leq i, j \leq 3$$

at the corresponding corner;

- the just mentioned control points $\mathbf{q}_{i,j}^9$ are fixed using the M-patch:
 - (a) the reparametrization γ^{R+1} from Section 4.1 corresponding to the same sector as G_Q^s is selected;
 - (b) the composition $F \circ \gamma^{R+1}$ is subdivided into four;
 - (c) the control points $\mathbf{q}_{i,j}^9$ are calculated to match the compositions;
- The auxiliary patch of bidegree (9, 9) is degree-raised to bidegree (11, 11); its 36 inner control points (with indices ij , $3 \leq i, j \leq 8$) are taken as the inner control points \mathbf{q}_{ij} of G_Q^s .

Remark 3. The order 1 part of a tensor-border structure of an extraordinary patch is of degree 9. Hence no information is lost when an auxiliary patch of bidegree (9, 9) is built. The remaining tensor-border structure is defined either by the piecewise mapping PW_7 of degree 7 or by adjacent ordinary patches of bidegree (5, 5). Thus the tensor-border of an extraordinary patch is controlled by the auxiliary patch. An auxiliary patch of bidegree (9, 9) simplifies the implementation of the algorithm since only partial derivatives of lower order must be calculated for the guide surface.

5 Conclusion

We have presented the construction of a polynomial C^2 spline surface that approximates a rational multi-sided M-patch. The key of the approach is the construction of a C^2 reparametrization to transmit the data of a guiding M-patch to the spline surface.

The method can be applied to other surfaces, not necessarily rational and it can be used to construct an infinite sequence of annuli in the spirit of subdivision algorithms.

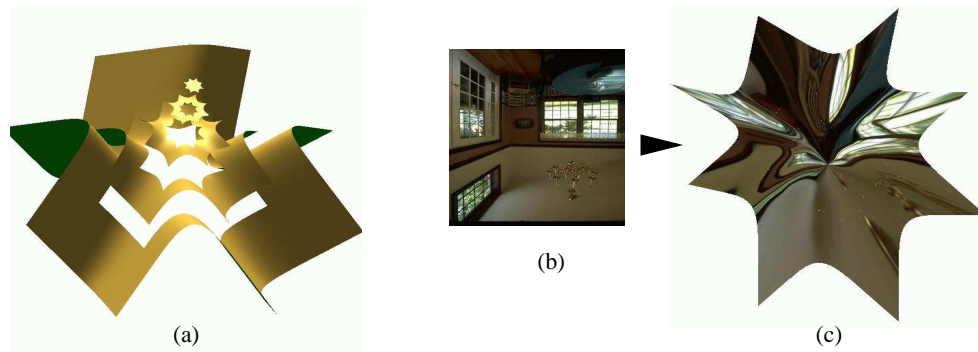


Fig. 13. A sample surface based on an unsymmetric monkey saddle and valence $m = 8$. (a) shows the initial data, three annuli of bidegree (5,5) and the cap of bidegree (11,11). (b) is a bitmap placed as an environment map onto the surface (c); of course only interactive, detailed (sectional) curvature analysis and reflection lines can establish the claim of good shape which, in turn, depends on the assumption that the M-patch has good shape.

References

1. de Boor, C.: B-Form Basics. In Gerald Farin, editor, *Geometric Modeling : Algorithms and New Trends*, pages 131–148, Philadelphia, 1987. SIAM.
2. Catmull, E., Clark, J.: Recursively generated B-spline surfaces on arbitrary topological meshes. *Computer Aided Design* **10**, 350–355. (1978).
3. Farin, G.: 1997. *Curves and Surfaces for Computer-Aided Geometric Design: A Practical Guide*, 4th Edition. Academic Press, New York, NY, USA.
4. Gregory, J., Zhou, J.: Irregular C^2 surface construction using bi-polynomial rectangular patches. *Computer Aided Geometric Design* **16** (1999) 424–435
5. Karčiauskas, K.: Rational M -patches and tensor-border patches. *Contemporary mathematics* **334** (2003) 101–128
6. Karčiauskas, K., Peters, J., Reif, U.: Shape characterization of subdivision surfaces – Case studies. to appear in *CAGD*
7. Peters, J.: C^2 free-form surfaces of degree (3, 5). *Computer Aided Geometric Design* **19** (2002) 113–126
8. Peters, J., Reif, U.: Analysis of generalized B -spline subdivision algorithms. *SIAM Journal on Numerical Analysis* **35** (1998) 728–748
9. Peters, J., Reif, U.: Shape characterization of subdivision surfaces – Basic principles. to appear in *CAGD*
10. Peters, J.: Smoothness, Fairness and the need for better multi-sided patches. *Contemporary mathematics* **334** (2003) 55–64.
11. Prautzsch, H.: Freeform splines. *Comput. Aided Geom. Design*, 14(3):201–206, 1997.
12. Prautzsch H., Boehm, W., Paluszny, M.: Bézier and B-spline techniques. Springer Verlag, Berlin, Heidelberg. (2002)
13. Reif, U.: TURBS—topologically unrestricted rational B -splines. *Constr. Approx.*, 14(1):57–77, 1998.